

OPTIMIZATION APPROACH FOR EFFICIENT CLEANING WITH IMPINGING JETS – INFLUENCE OF NOZZLE DIAMETER, PRESSURE AND NOZZLE DISTANCE

H. Köhler¹, H. Stoye¹, M. Mauermann² and J.-P. Majschak^{1,2}

¹ Technische Universität Dresden, Faculty of Mechanical Engineering, Institute of Processing Machines and Mobile Machines, Bergstr. 120, 01062 Dresden, Germany, hannes.koehler@tu-dresden.de

² Fraunhofer IVV, Branch Lab for Processing Machinery and Packaging Technology AVV, Heidelberger Str. 20, 01189 Dresden, Germany

ABSTRACT

Efficient cleaning is a considerable challenge in various industrial fields. Laboratory scale cleaning tests are an approach to investigate the influences of operating parameters on the cleaning result and to assess the required efforts. In this paper an impinging jet cleaning process was studied. The test set-up and evaluation method enables the measuring of the circular area cleaned by the jet as a function of time. Cleaning tests with a food based model soil were carried out under variation of the most relevant industrial operating parameters: nozzle diameter (0.39 to 3.30 mm), pressure (0.1 to 5.0 bar) and nozzle distance (16 to 184 mm). The first two parameters showed a power-law dependency, while the latter was neglected due to the coherent jet structure. A semi-empirical model is presented which can be used to optimize the cleaning process. Different process-related boundary conditions lead to different optimal solutions, e.g. to minimize the cleaning time, fluid consumption or the total cleaning costs.

INTRODUCTION

Clean surfaces are a major prerequisite for efficient industrial processes, e.g. for optimal heat transfer in heat exchangers or for the hygienic production of high quality food products. An optimization of cleaning processes requires knowledge of the relation between operating parameters and cleaning result. Subsequently, the required efforts are essential in assessing the cleaning efficiency. The most common industrial assessment criteria are cleaning time and the amount of cleaning fluid consumed. The related costs vary over a wide range depending on the branch of industry and the company in particular. Freshwater costs range from 0.19 - 2.30 €/m³ in the brewery industry (Hien et al., 2008) or up to 4 €/m³ in the pharmaceutical industry (Graf, 2010). Additional waste water costs can reach amounts up to 300 €/m³ if hormones or carcinogenic substances are present (Eckert et al., 2012). The time-related costs for the loss of production due to cleaning vary likewise and depend on each individual case. This infers that an optimization should take into account these application-specific costs for the efforts to find the

optimal operating parameters which bring out a minimum of total costs under the given boundary conditions.

Water jets are commonly used for cleaning of large surfaces, e.g. for plate heat exchanger or rotary jet heads for tank cleaning in food and marine industries (Müller-Steinhagen, 2000; Tamime, 2009). There are two main types of water jet. The first, droplet jets, is where the jet is transformed into droplets and individual droplets hit the surface. The second, coherent jets, occurs when a fluid column impinges and spreads out radially. In the literature the former is often labeled as ‘impinging jet’ and is in the focus of this work.

An overview of the characteristics of impinging jet cleaning is given by Detry et al. (2009). The main operating parameters which are independently adjustable by the operator are in case of a stationary, round jet the nozzle diameter, D , the gauge pressure, p , and the distance between the nozzle exit and the surface to be cleaned (nozzle distance, a). The first two result in a specific volume flow rate, Q , calculable by Eq. (1) for inviscid flow.

$$Q = \frac{\pi}{4} D^2 \cdot \sqrt{\frac{2p}{\rho}} \quad (1)$$

These parameters, in combination with the fluid properties, determine the flow conditions on the surface. Extensive research has been done to describe the flow field and the position of the hydraulic jump, r_{jump} , of impinging jets on unsoiled surfaces (Watson, 1964; Middleman, 1995; Wilson et al., 2012; Wang et al., 2013). The soil removal is influenced by the interaction of cleaning fluid, characterized by the flow specific parameters (e.g. local shear stress), and the soil. The underlying mechanism(s) are complex and subject of current research (Gillham et al., 1999; Jensen and Friis, 2004; Fryer and Asteriadou, 2009; Schöler et al., 2012).

Soil removal by coherent jets ($9.7 \times 10^3 \leq Re_{\text{Nozzle}} \leq 2.0 \times 10^4$) has been investigated by Yeckel and Middleman (1987) for thin, insoluble, viscous silicone oil films. They measured the mean decrease of residual film thickness within a certain radius at discrete time steps. Their model, based on the Reynolds’ lubrication approximations,

predicted the film thinning effectively for longer flushing times. Examinations concerning the spatial progress of the cleaning were limited to their experimental techniques by differential weighing. Further studies examining the spatial and time related cleaning progress of a non-submerged impinging jet are not known to the authors.

Leu et al. (1998) and Meng et al. (1998) conducted cleaning experiments using stationary and moving water jets with various operating parameters. The high pressure of the water jet ($6.6 \times 10^4 \leq Re_{\text{Nozzle}} \leq 2.6 \times 10^5$) leads to atomization of the jet, starting near the nozzle exit. Droplet velocity, size and lateral distribution changed with increased standoff distance. They analyzed and modeled paint removal with the assumption that removal occurs when a certain fatigue limit of the soil is exceeded due to the impinging stress of single droplets (water hammer effect) – underlying only cohesive failure. Their results indicated a linear dependency of the cleaned width to the nozzle diameter and a pressure dependency to the power of 0.25. The time influence was only considered to moving jets. The cleaned width is then reciprocally proportional to the jet velocity and the exponents for the diameter and pressure influence were extended with an empirical, probably material dependent, constant.

As long as the cleaning mechanism(s) are not completely understood, laboratory scale cleaning tests and empirical modeling can help to design efficient cleaning processes. Latest research enabled a direct spatial- and time-resolved measuring of the cleaning progress by using optical methods (Schöler et al., 2009; Mauermann, 2012).

Therefore the objectives of this paper are:

- development of a method in laboratory scale to assess cleaning by impinging jets spatial- and time-resolved
- measurement of the influences of the operating parameters in order to provide data for further analysis
- development of a semi-empirical model of these influences exemplary for one model food soil
- development of an approach to optimize the cleaning process application-specific.

EXPERIMENTAL TECHNIQUES

Soiling procedure

The model food soil is the polysaccharide Xanthan gum (Kremer Pigmente GmbH & Co. KG, Xanthan, CAS 11138-66-2) mixed with 3% (w/v) crystalline zinc sulfide (Honeywell, USA, Lumilux® Effect Green N-FF) as optical tracer. The Xanthan gum (0.5% w/v) was dissolved in distilled water (23°C) under stirring by 600 rpm. After 30 minutes the tracer was added.

The test metal sheets (500x500x1 mm, AISI 304 2B) were pre-cleaned before soiling with water and ethanol. For soiling the sheets were placed in an upright position and the test soil was sprayed on homogeneously.

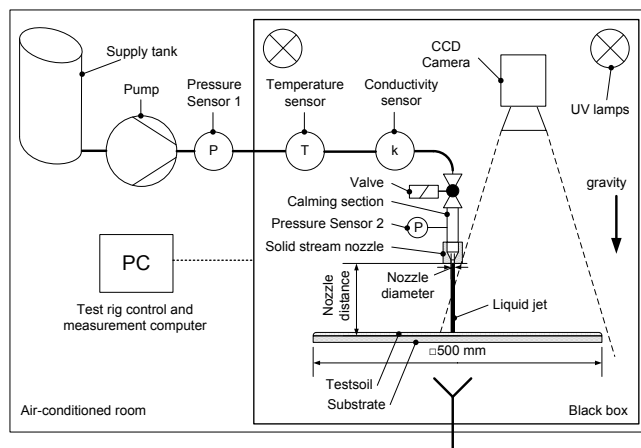


Fig. 1 Cleaning test rig with online monitoring system

The excess solution flows down by retaining a thin homogeneous soil film on the sheet. Afterwards the sheets dried at room temperature for 24h resulting in a mean surface mass of $m_0 = 1.3 \pm 0.1 \text{ mg/cm}^2$.

Cleaning test rig

For cleaning the test rig shown in Fig. 1 was used. A test metal sheet is continuously cleaned for 10 minutes by a vertical, round, stationary, coherent, perpendicular impinging, liquid jet while the cleaning progress is captured online with a CCD-Camera (MATRIX VISION GmbH, mvBlueCOUGAR-X125aG, 5 Mpx gray-sensor, 14 bit). The liquid jet is generated by solid stream nozzles (Lechler GmbH, Type 544). Different nozzle diameters were used (Table 1). Furthermore the nozzle distance and the pressure can be adjusted. The test metal sheet is horizontally placed in the middle under the nozzle with an inclination ($< 1^\circ$) to ensure unchanging flowing off the sheet. The phosphorescent tracer within the soil is illuminated by two UV lamps. To maintain constant the light conditions during the cleaning, the set up was surrounded by a black box to shield from additional light. The experiment is controlled by a computer, which regulates the pump pressure, opens the valve, triggers the camera and records sensor data. Before the valve opens a first photo of the test sheet is captured under dry conditions.

Data analysis

All acquired images of an experiment were automatically analyzed by a MATLAB® script. The images were cropped, the region of interest (ROI) with a resolution of 40×1780 pixels, located adjacent to the impinging point as implied in Fig. 2(a). Mean value and standard deviation were calculated over 40 pixels in the lateral direction. No averaging was made in radial direction to retain full spatial resolution (0.14 mm/pixel). These intensity, I , over radius, r , curves of every image were standardized to the initial dry intensity curve. Fig. 2(b) shows an example of a normalized intensity curve at time $t = 200 \text{ s}$.

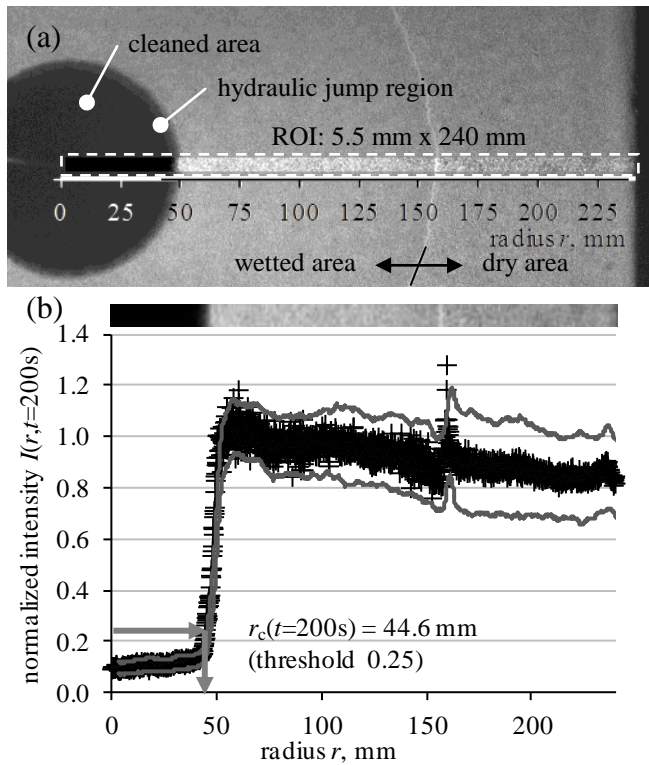


Fig. 2 Data analysis as an example at time $t=200$ s (a) reduced sample picture with ROI and manually adjusted contrast for better visualization; (b) out of the ROI generated graph showing normalized intensity vs. radius with standard variation limits

The cleaned area exhibits a very low intensity (Schöler et al., 2012). In the soiled area the normalized intensity values can exceed one due to reflections, soil accumulation or the liquid-gaseous phase boundary (referring to $r \approx 160$ mm). The reduced intensity of the unaffected soil layer ($r > 160$ mm) is due to absorption of unavoidable mist occurring during cleaning. Investigations showed that these had negligible influence on the determination of the cleaned radius, r_c . The radius is assigned to r_c where the normalized intensity exceed a defined threshold for first occurrence (Fig. 2(b)). Extensive research has been done to obtain a valuable threshold. Therefore the cleaned radii of nine cleaning experiments with different parameters were manually measured at seven different times using the ruler tool of a graphics editor. These manually obtained radii were compared with the cleaned radii which were automatically determined by different thresholds. Then the correlation coefficient and relative error between both were calculated to assess the thresholds. The threshold-value 0.25 turned out to be suitable and robust ($R^2=0.9965$; rel. error=2%). By means of the threshold and automatic analysis of the images the so called ‘cleaning-curves’ – cleaned radius r_c plotted versus time can be obtained. Three typical cleaning-curves are shown in Fig. 3. In this work we evaluated the cleaned radii at the discrete points in time $t = \{10, 30, 60, 120, 450\}$ s for the further analysis.

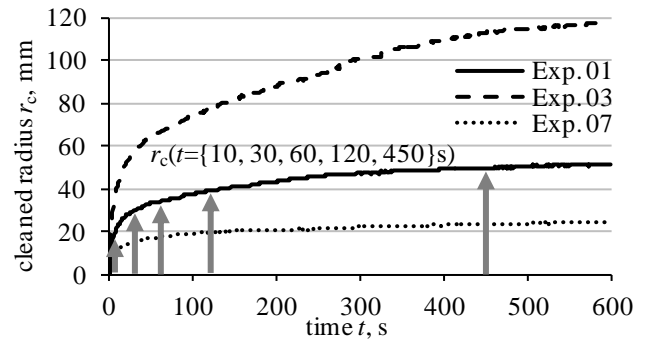


Fig. 3 Typical cleaning-curves for three experiments with evaluated cleaned radii at discrete time steps

Experiments

27 experiments with 126 valid runs were conducted by four different operators. For all experiments the cleaning fluid was purified water ($17 \pm 4^\circ\text{C}$). The operating parameters nozzle diameter, D , pressure, p , and nozzle distance, a , were varied by using the design of experiments principles and are listed in a sorted order in Table 1 showing real and normalized values ($6.7 \times 10^3 \leq Re_{\text{Nozzle}} \leq 5.7 \times 10^4$).

RESULTS

Cleaning progress in relation to the hydraulic jump

The values of the hydraulic jump radii, r_{jump} , were measured with a ruler on an unsoiled sheet. For higher volume flow rates the position fluctuated more strongly. No accurate position was determinable for experiments 21 and 22. In Fig. 4 the cleaned radii for 10, 60 and 450 s are plotted against r_{jump} . The correlation coefficient between r_c and r_{jump} is approximately 0.95 for all time steps. With increasing time r_c converges to r_{jump} . Subsequently r_c exceeds r_{jump} but stagnates within the region behind r_{jump} .

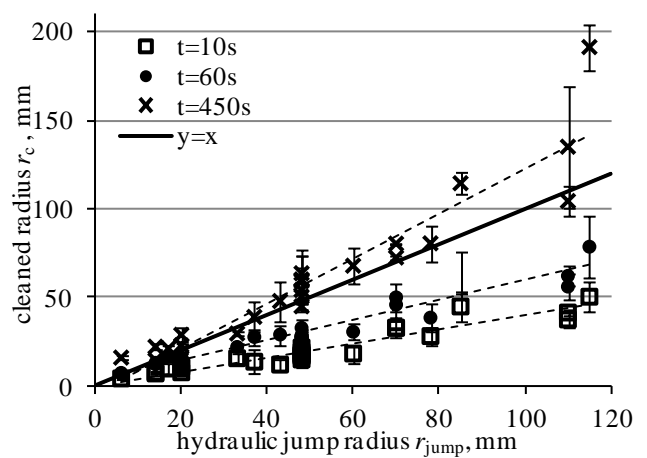


Fig. 4 Relation of cleaned radius to the radius of the hydraulic jump for different time steps; dashed lines indicate linear regressions

Table 1 Experiments conducted, radius of hydraulic jump and results as cleaned radii in mm for five time steps. Bold lines separate the center, full factorial and axial experiments based on the design of experiments principles.

Exp.	qty.	D , mm	p , bar	a , mm	D^*	p^*	a^*	r_{jump} , mm	$r_c(t)$, mm				
								unsoiled	$t=10\text{s}$	$t=30\text{s}$	$t=60\text{s}$	$t=120\text{s}$	$t=450\text{s}$
01	24	1.69	1.5	100	-0.1	0	0	48	22 ± 3	28 ± 4	33 ± 5	38 ± 5	50 ± 4
02	3	2.66	2.0	150	1	1	1	110	38 ± 4	46 ± 3	56 ± 7	72 ± 13	135 ± 35
03	4	2.66	2.0	50	1	1	-1	110	41 ± 2	54 ± 4	62 ± 6	71 ± 7	104 ± 8
04	3	2.66	1.0	150	1	-1	1	70	33 ± 5	39 ± 7	46 ± 7	52 ± 8	80 ± 0
05	3	2.66	1.0	50	1	-1	-1	70	33 ± 0	43 ± 5	50 ± 7	56 ± 10	72 ± 2
06	3	0.84	2.0	150	-1	1	1	20	11 ± 1	14 ± 1	16 ± 0	19 ± 1	29 ± 4
07	4	0.84	2.0	50	-1	1	-1	20	11 ± 2	14 ± 2	16 ± 3	18 ± 3	23 ± 2
08	3	0.84	1.0	150	-1	-1	1	14	8 ± 1	11 ± 0	13 ± 0	16 ± 1	22 ± 1
09	3	0.84	1.0	50	-1	-1	-1	14	7 ± 1	11 ± 2	12 ± 1	13 ± 1	15 ± 1
10	2	0.39	1.5	100	-1.5	0	0	6	4 ± 0	6 ± 0	7 ± 0	8 ± 1	16 ± 1
11	3	0.84	1.5	100	-1.0	0	0	17	10 ± 3	14 ± 3	17 ± 2	20 ± 0	21 ± 2
12	4	2.66	1.5	100	1.0	0	0	85	45 ± 8	53 ± 11	64 ± 12	80 ± 16	114 ± 6
13	3	3.30	1.5	100	1.7	0	0	115	50 ± 8	63 ± 14	79 ± 18	103 ± 13	191 ± 13
14	3	1.69	0.1	100	-0.1	-2.8	0	20	8 ± 1	9 ± 2	11 ± 1	15 ± 1	16 ± 0
15	3	1.69	0.5	100	-0.1	-2.0	0	33	16 ± 3	20 ± 2	22 ± 2	25 ± 2	30 ± 1
16	3	1.69	0.7	100	-0.1	-1.7	0	37	14 ± 7	22 ± 5	28 ± 4	31 ± 3	39 ± 8
17	3	1.69	1.0	100	-0.1	-1.0	0	43	12 ± 3	22 ± 3	29 ± 6	36 ± 4	48 ± 11
18	8	1.69	2.0	100	-0.1	1.0	0	48	18 ± 5	23 ± 4	27 ± 3	34 ± 6	60 ± 14
19	6	1.69	2.3	100	-0.1	1.7	0	60	18 ± 5	24 ± 4	31 ± 5	39 ± 5	68 ± 10
20	3	1.69	3.0	100	-0.1	3.0	0	78	28 ± 5	34 ± 6	39 ± 8	46 ± 8	80 ± 10
21	3	1.69	4.0	100	-0.1	5.0	0	<i>n/a</i>	29 ± 7	36 ± 10	43 ± 10	56 ± 13	105 ± 11
22	3	1.69	5.0	100	-0.1	7.0	0	<i>n/a</i>	28 ± 7	36 ± 11	45 ± 12	61 ± 14	124 ± 10
23	5	1.69	1.5	16	-0.1	0	-1.7	48	15 ± 2	22 ± 3	28 ± 3	35 ± 4	60 ± 16
24	3	1.69	1.5	33	-0.1	0	-1.3	48	19 ± 1	23 ± 0	27 ± 0	34 ± 2	45 ± 2
25	7	1.69	1.5	50	-0.1	0	-1.0	48	17 ± 6	24 ± 4	28 ± 4	35 ± 4	54 ± 12
26	8	1.69	1.5	150	-0.1	0	1.0	48	18 ± 3	23 ± 2	28 ± 3	36 ± 4	64 ± 10
27	6	1.69	1.5	184	-0.1	0	1.7	48	17 ± 3	22 ± 5	27 ± 3	34 ± 3	59 ± 2

Influence of nozzle distance

Figure 5 shows that the cleaned radius for a coherent water jet is unaffected by the nozzle distance within the investigated range. This is valid for all investigated time steps (refer also to Table 1, Exp. 23-27). The values for 450 s show noticeably larger variations.

Influence of nozzle diameter and pressure

Figure 6 shows the results for the nozzle diameter and pressure for $t=30\text{s}$ in a log-log-plot exemplary for the other time steps. The linear correlation for both parameters shows that each influence could be well described by power-law. The associated parameters factor c and exponent α were determined for all time steps. Table 2 indicates that the exponents are time-independent. Higher variations occur in particular for the pressure influence at $t=450\text{s}$.

Modeling of the cleaning effects

On the basis of the univariate experiments 10-27 a semi-empirical model Eq. (2) was developed. In addition the time influence is integrated. Most log-log-plots (not shown) of the cleaning-curves (Fig. 3) indicate the application of the

power-law also for the cleaning progress. The parameters in Eq. (2) were determined by using only the data of the experiments 01 to 09 to show that a) the model parameters obtained in this way are also valid for experiments further away from the center and b) these small number of experiments are sufficient enough to obtain the model parameters, for another soil.

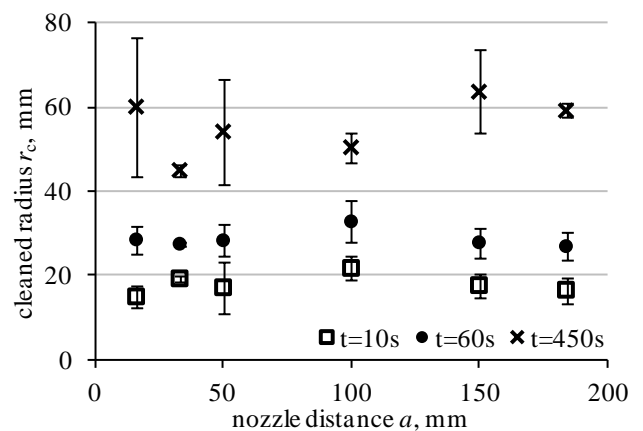


Fig. 5 Influence of nozzle distance on cleaned radius for different time steps

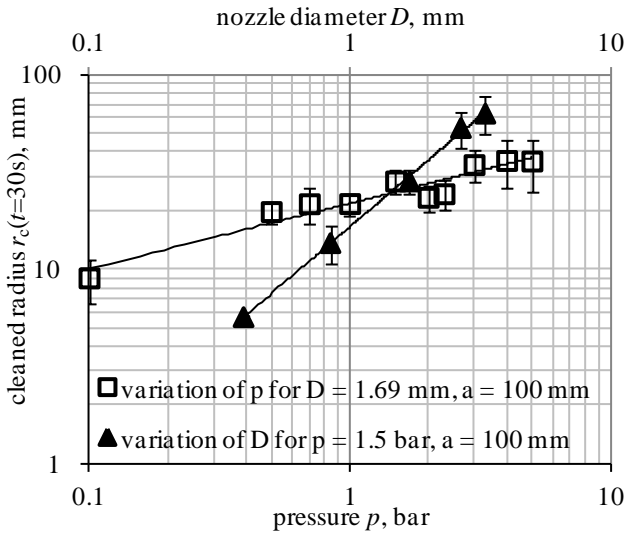


Fig. 6 Log-log-plot of the dependency of the cleaned radius r_c at $t=30s$ on nozzle diameter D and pressure p

The fitting was done in MATLAB® R2010a using the function *nlinfit* with options 'Robust', 'on', 'WgtFun', 'bisquare' in order to reduce the influence of outliers. The cleaned radii calculated by Eq. (2) vs. the measured values are plotted in Fig. 7. Larger deviations from the 1:1 ratio occur at shorter (10s) and larger (450s) time steps. Cleaned radii measured prior to 10s showed high variations between individual runs and are therefore not considered.

$$r_c / \text{mm} = 6.3349 \cdot D / \text{mm}^{1.1751} \cdot p / \text{bar}^{0.3779} \cdot t / \text{s}^{0.212} \quad (2)$$

DISCUSSION

Discussion of the results and the semi-empirical model

Nozzles for droplet sprays have an optimum of their cleaning performance at a certain distance (Leu et al., 1998; Meng et al., 1998; Mauermann, 2012). In contrast this influence could not be confirmed here within the examined range of distance for the solid stream nozzles (Fig. 5). The independence of distance is related to the coherent structure of the jet. This in turn is strongly linked to the nozzle design (Reitz and Bracco, 1982; Dumouchel, 2008). This is advantageous for designing the cleaning process since this parameter could be neglected although the nozzle design should receive more attention.

The nozzle diameter and pressure influences are consistent with the power-law relations of Leu et al. and Meng et al. The independence of time of both parameters simplifies the semi-empirical model. Qualitative observations and unpublished preliminary fluid dynamic gauging measurements assume a very fast hydration and swelling of the Xanthan gum within a few seconds.

Table 2 Parameters of power-law for nozzle diameter and pressure influence for all time steps

t, s	nozzle diameter $r_c=c_1 \cdot D^\alpha$			pressure $r_c=c_2 \cdot p^\alpha$		
	$c_1, 1/\text{mm}^{\alpha-1}$	α	R^2	$c_2, \text{mm}/\text{bar}^\alpha$	α	R^2
10	12.6	1.190	0.995	16.3	0.339	0.8513
30	16.4	1.139	0.998	21.7	0.336	0.9173
60	20.3	1.113	0.996	26.6	0.326	0.9234
120	24.1	1.170	0.993	32.4	0.340	0.9449
450	35.9	1.164	0.924	46.5	0.517	0.9748

To gain deeper understanding of the cleaning process these effects have to be investigated more in detail.

Figure 7 indicates that the semi-empirical model, parameterized by Exp. 01 to 09 fits reasonably accurate over the whole operating parameter area. Furthermore only five experiments should be sufficient to determine the model parameters since the number of experiments (02 to 09) can be halved by neglecting the influence of distance (Table 1, Fig. 5). The variations can result from the conducting operator, especially concerning to the soiling and drying process. At 450s the variations resulted due to the temperature, revealed by examining the individual runs. Further investigations over a wider range are planned when a heater and temperature control are installed in the test rig. The flow conditions within the hydraulic jump region may have an effect when the cleaned radius converges (Fig. 4). Furthermore different jump forms as described by Liu and Lienhard (1993) were observed. This may also effect the results. The present detection method is not able to determine the hydraulic jump during a cleaning experiment. Operator observations during the cleaning process give rise to the hypothesis that the jump position is even influenced by the cleaning progress. Therefore, the presented model (particularly the time factor) could be only valid till the cleaned radius reaches the hydraulic jump.

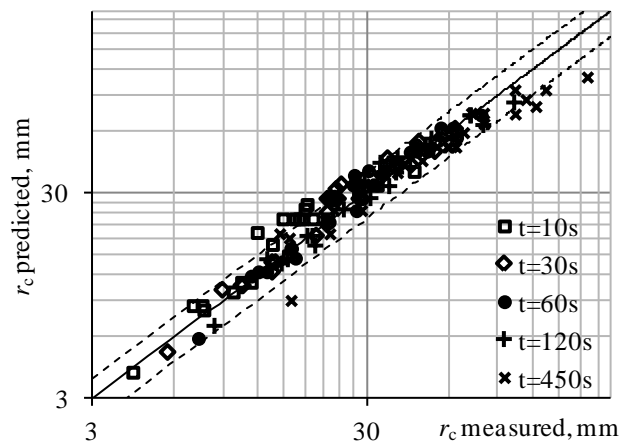


Fig. 7 Comparison of predicted (Eq. (2)) and measured cleaned radii for all time steps. Dashed lines indicate a range of deviation up to 25%

Evaluation in terms of the cleaning rate

The semi-empirical model could be further used to evaluate the cleaning process by means of the cleaning rate. The cleaning rate describes the removed amount of soil with time (Schlüßler, 1970) and therefore it can be applied e.g. to compare different cleaning processes or to relate the cleaning result to the efforts. The discrete cleaning rate \overline{R}_d is related to a specific point in time, while the main cleaning rate describes a mean cleaning speed from the beginning to the end of cleaning (Bode et al., 2005). Here the discrete cleaning rate can be calculated with the surface mass and the cleaned area according to Eq. (3).

$$\overline{R}_d = \frac{m_0 \cdot \partial(\pi \cdot r_c(D, p, t)^2)}{\partial t} \quad (3)$$

The dependency of the discrete cleaning rate on time is here proportional to the power of -0.58 – this implies that the cleaning rate is strictly monotonically decreasing. Further on the cleaning rate exponents for the nozzle diameter are 2.35 and for the pressure 0.76 – both are greater than these for the volume flow rate (Eq. (1)). This infers that cleaning a certain area (within the hydraulic jump) of this test soil by a stationary jet could be achieved with a minimum of cleaning fluid and time when diameter and pressure are maximized.

OPTIMIZATION APPROACH

Basic idea

The following considerations should demonstrate an approach to use the semi-empirical model to find the optimal operating parameters under application-specific boundary conditions for an impinging jet cleaning process. The experimental validation is still outstanding and part of ongoing research.

The cleaning task is defined as shown in Fig. 8. An even plate with rectangular shape and dimension width, w , and height, h , should be cleaned by a meandering impinging jet with a constant speed, v_{jet} .

The following assumptions are made:

- the soil properties, including thickness, are homogeneous over the plate
- no soil weakening due to a drainage film is considered
- side effects and a final rinse step to wash down loose soil residuals are neglected
- the nozzle diameter and pressure influences for the stationary jet are applicable to a moving jet (unpublished preliminary examinations suggest this assumption).

The track distance, d_{track} , can therefore be calculated according to Eq. (4) with an additional safety factor, S (0...100 %), for track overlapping.

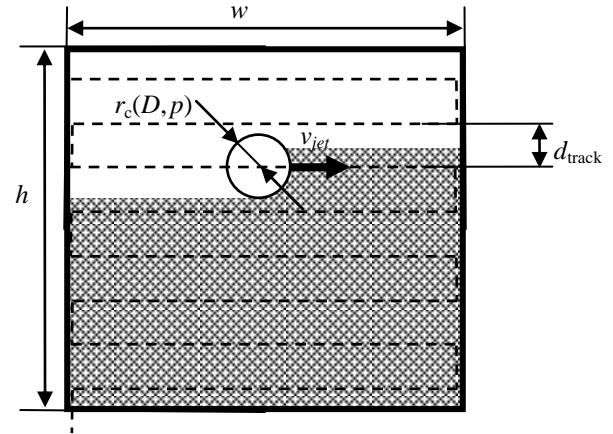


Fig. 8 Possible cleaning task

$$d_{track}(D, p) = 2 \cdot r_c(D, p) \cdot (1 - S) \quad (4)$$

The total cleaning time, t_{total} , and total fluid consumption, V_{total} , can further be approximated as follows:

$$t_{total}(D, p) = \frac{h}{v_{jet}} \cdot w \quad (5)$$

$$V_{total}(D, p) = Q(D, p) \cdot t_{total}(D, p) \quad (6)$$

By introducing application-specific cost rates per time, CR_t , and volume cleaning fluid, CR_V , it is possible to calculate the total costs, TC , for the whole cleaning task:

$$TC(D, p) = CR_t \cdot t_{total}(D, p) + CR_V \cdot V_{total}(D, p) \quad (7)$$

The cost rate per volume could take e.g. fresh and waste water, chemicals and heating costs into account. The costs for loss of production or electricity for pumps can be covered by the time related cost rate. These cost rates should be provided by the management accounting. Thus it is possible to solve the minimizing problem within the process related boundary conditions.

Considerations by example

The last assumption implies that the cleaned track width of a moving jet with a constant speed could be related to a cleaned radius at a discrete time step. Therefore the following calculations were conducted with a cleaned radius dependency for $t=120$ s, a jet moving speed of 10mm/s and a track overlapping factor S of 25% for a test sheet with $w=h=500$ mm. These values are chosen based on unpublished preliminary examinations to demonstrate the relations between the operating parameters ($0.39 \text{ mm} \leq D \leq 3.3 \text{ mm}$; $0.1 \text{ bar} \leq p \leq 5 \text{ bar}$) and the cleaning results (total cleaning time, fluid consumption and costs).

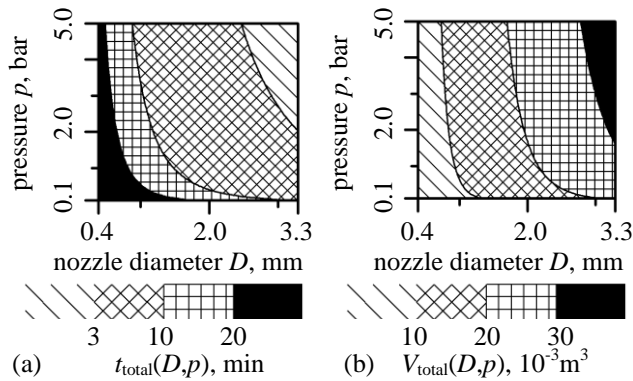


Fig. 9 Dependency of (a) total cleaning time t_{total} (Eq. (5)) and (b) total fluid consumption V_{total} (Eq. (6)) on nozzle diameter and pressure for numerical values given in the text, shadings represent values between the given limits in the legend below

As shown in Fig. 9 both optima are located in opposite corners: a minimum of cleaning time is achieved by the greatest nozzle diameter and greatest pressure and vice versa for a minimum of fluid volume.

The optimal operating parameters depend on the individual application-specific cost rates and can be determined by considering the total costs as shown in Fig. 10, as an example for $CR_t=24\text{€}/\text{h}$ and $CR_v=150\text{€}/\text{m}^3$. An optimal solution can be found for $D=1.6\text{mm}$ and $p=5\text{bar}$.

CONCLUSIONS / OUTLOOK

1. The optical detection and analysis method presented in this paper is suitable to determine spatial- and time-resolved cleaning effects by impinging jets in terms of 'cleaning curves', providing that a significant contrast between soiled and unsoiled areas exists.
2. A semi-empirical model for the cleaned radius is presented which describes the dependencies of nozzle diameter, pressure and cleaning time reasonably accurate. For coherent jets the nozzle distance could be neglected within certain limits. The – soil dependent – model parameters could be determined by conducting five experiments. The improvement of the prediction accuracy is part of ongoing research.
3. The model is a promising approach to assess the cleaning efficiency for different application cases. Due to the possibility to predict the cleaning result and the efforts it can be used to determine application-specific the most efficient operating parameters under given boundary conditions. Further on additional interactions, like the jet moving speed, could be implemented in the model. Additionally it is possible to analyze the parameter sensitivity on the one hand to check the robustness of the process and on the other hand to assess potential for savings.

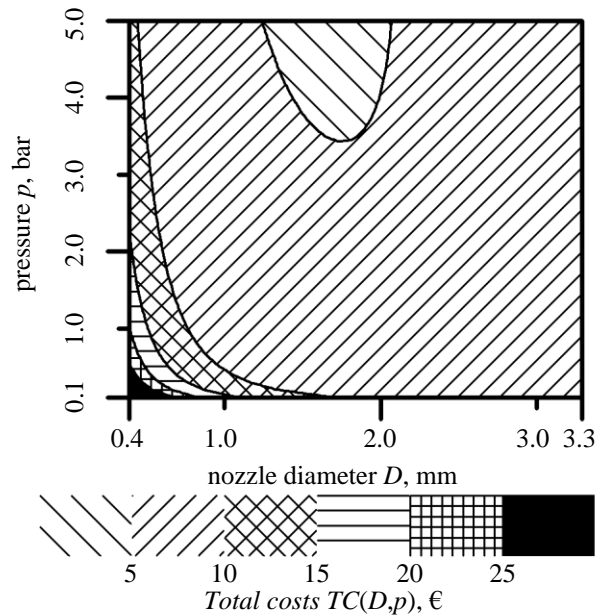


Fig. 10 Dependency of total costs (Eq. (7)) on nozzle diameter and pressure for exemplary numerical values given in the text, shadings represent values between the given limits in the legend below

4. The possibility to predict the cleaned width of moving jets enables a soil-specific adaptation of the gear ratio of rotary jet heads as a first aspect. Prospective the usage of programmable cleaning devices is required to turn the optimization approach fully into practice.
5. The different dependencies as described by the model could be further used in combination with a suitable monitoring system as a cleaning process control. Deviations from the expected cleaned width, e.g. due to variations in the soil amount, soil weakening due to a drainage film or undetected pressure decrease through leakage during cleaning can be readjusted by inline changes of pressure or moving speed. The implementation of this model in a self-learning control system for cleaning should be a long-term objective.

NOMENCLATURE

a	distance, m
c	power-law factor, various unit
CR	cost rate, €/various unit
d	distance, m
D	nozzle diameter, m
h	height, m
I	normalized intensity, dimensionless
m_0	initial surface mass, kg/m^2
p	gauge pressure, kg/m^2
Q	volume flow rate, m^3/s
r	radius, m
R^2	correlation coefficient, dimensionless
\bar{R}_d	discrete cleaning rate, g/s
Re	Reynolds number, uD/v , dimensionless

S	safety factor, %
t	time, s
TC	total costs, €
u	velocity, $\sqrt{(2p/\rho)}$, m/s
v	moving speed, m/s
V	volume, m ³
w	width, m
α	power-law exponent, dimensionless
ν	kinematic viscosity, m ² /s
ρ	density, kg/m ³

Subscript

0	initial
c	cleaned
d	discrete
jet	jet
jump	hydraulic jump
nozzle	related to nozzle diameter
t	time
total	total
track	track
V	volume

Superscript

*	normalized values
---	-------------------

ACKNOWLEDGEMENT

This research project is supported by funds of the European Union and the Free State of Saxony (SAB 080951793).

REFERENCES

Bode, K., Hooper, R.J., Augustin, W., Paterson, W.R., Wilson, D.I., Scholl, S., 2005, Pulsed flow cleaning of whey protein fouling layers, *Proc. 6th Int. Conference on Heat Exchanger Fouling and Cleaning 2005*, Kloster Irsee, Germany, pp. 165-173.

Detry, J.G., Deroanne, C., Sindic, M., 2009, Hydrodynamic systems for assessing surface fouling, soil adherence and cleaning in laboratory installations, *Biotechnol. Agron. Soc. Environ.*, Vol. 13, pp. 427-439.

Dumouchel, C., 2008, On the experimental investigation on primary atomization of liquid streams, *Exp. Fluids*, Vol. 45, pp. 371-422.

Eckert, V., Bensmann, H., Zegenhagen, F., Weckenmann, J., Sörensen, M., 2012, Elimination of Hormones in Pharmaceutical Waste Water, *Pharm. Ind.*, Vol. 74, pp. 487-492.

Fryer, P.J., Asteriadou, K., 2009, A prototype cleaning map: A classification of industrial cleaning processes, *Trends Food Sci. Technol.*, Vol. 20, pp. 255-262.

Gillham, C.R., Fryer, P.J., Hasting, A.P.M., Wilson, D.I., 1999, Cleaning-in-Place of Whey Protein Fouling Deposits: Mechanisms Controlling Cleaning, *Food Bioprod. Process.*, Vol. 77, pp. 127-136.

Graf, C., 2010, Energieeffiziente Herstellung von Pharmawasser, *Pharm. Ind.*, Vol. 72, pp. 1797-1803.

Hien, O., K pferling, E., Guggeis, H., 2008, Wassermanagement in der Getr nkeindustrie, *BRAUWELT*, Vol. 23, pp. 640-643.

Jensen, B.B.B., Friis, A., 2004, Critical wall shear stress for the EHEDG test method, *Chem. Eng. Process. Process Intensif.*, Vol. 43, pp. 831-840.

Leu, M.C., Meng, P., Geskin, E.S., Tismeneskiy, L., 1998, Mathematical modeling and experimental verification of stationary waterjet cleaning process, *J. Manuf. Sci. Eng.*, Vol. 120, pp. 571-579.

Liu, X., Lienhard, J.H., 1993, The hydraulic jump in circular jet impingement and in other thin liquid films, *Exp. Fluids*, Vol. 15, pp. 108-116.

Mauermann, M., 2012, *Methode zur Analyse von Reinigungsprozessen in nicht immersierten Systemen der Lebensmittelindustrie*, Technische Universit t Dresden, Thesis.

Meng, P., Geskin, E.S., Leu, M.C., Li, F., Tismeneskiy, L., 1998, An analytical and experimental study of cleaning with moving waterjets, *J. Manuf. Sci. Eng.*, Vol. 120, pp. 580-589.

Middleman, S., 1995, *Modeling Axisymmetric Flows: Dynamics of Films, Jets, and Drops*, Academic Press, Burlington.

M ller-Steinhagen, H., 2000, *Heat Exchanger Fouling: Mitigation and Cleaning Technologies*, PUBLICO, Essen.

Reitz, R.D., Bracco, F.V., 1982, Mechanism of atomization of a liquid jet, *Phys. Fluids*, Vol. 25, pp. 1730-1742.

Schl bler, H.-J., 1970, Zur Reinigung fester Oberfl chen in der Lebensmittelindustrie, *Milchwissenschaft*, Vol. 25, pp. 133-145.

Sch ler, M., F ste, H., Helbig, M., Gottwald, A., Friedrichs, J., Werner, C., Augustin, W., Scholl, S., Majschak, J.-P., 2012, Local analysis of cleaning mechanisms in CIP processes, *Food Bioprod. Process.*, Vol. 90, pp. 858-866.

Sch ler, M., Fuchs, T., Helbig, M., Augustin, W., Scholl, S., Majschak, J.-P., 2009, Monitoring of the local cleaning efficiency of pulsed flow cleaning procedures, *Proc. 8th Int. Conference on Heat Exchanger Fouling and Cleaning 2009*, Schladming, Austria, pp. 455-463.

Tamime, A.Y., 2009, *Cleaning-in-Place: Dairy, Food and Beverage Operations*, 3rd., Wiley-Blackwell, Hoboken.

Wang, T., Davidson, J.F., Wilson, D.I., 2013, Effect of surfactant on flow patterns and draining films created by a static horizontal liquid jet impinging on a vertical surface at low flow rates, *Chem. Eng. Sci.*, Vol. 88, pp. 79-94.

Watson, E.J., 1964, The radial spread of a liquid jet over a horiz. plane. *J. Fluid Mech.*, Vol. 20, pp. 481-499.

Wilson, D.I., Le, B.L., Dao, H.D.A., Lai, K.Y., Morison, K.R., Davidson, J.F., 2012, Surface flow and drainage films created by horizontal impinging liquid jets, *Chem. Eng. Sci.*, Vol. 68, pp. 449-460.

Yeckel, A., Middleman, S., 1987, Removal of a viscous film from a rigid plane surface by an impinging liquid jet, *Chem. Eng. Commun.*, Vol. 50, pp. 165-175.